Numerical discretizations for shallow water equations with source terms on unstructured meshes

Arnaud Duran

I3M, Montpellier, UMR CNRS 5149, France

Joint Work with F.Marche (I3M, Montpellier, UMR CNRS 5149, France)
Q.Liang (SCEG Newcastle, United Kingdom)
C.Berthon and R.Turpault (Laboratoire de Mathematiques Jean Leray, Université de Nantes, France)

HYP 2012

Plan

2D shallow water equations

$$u_t + \nabla.\mathcal{H}(u) = -\mathcal{B}(u,z) - \mathcal{F}(u), \quad with$$

$$u = \begin{pmatrix} h \\ q_x \\ q_y \end{pmatrix} \quad \mathcal{H}(u,z) = (F,G)(u,z) = \begin{pmatrix} q_x & q_y \\ \frac{q_x^2}{h} + \frac{1}{2}gh^2 & \frac{q_x q_y}{h} \\ \frac{q_x q_y}{h} & \frac{q_y^2}{h} + \frac{1}{2}gh^2 \end{pmatrix}$$

Source terms :

$$\mathcal{B}(u,z) = {}^t(0, gh\partial_x z, gh\partial_y z) \quad \mathcal{F}(u) = {}^t\left(0, \kappa\frac{\sqrt{q_x^2+q_y^2}}{h^\gamma}q_x, \kappa\frac{\sqrt{q_x^2+q_y^2}}{h^\gamma}q_y\right)$$

- h : water height
- η : free surface
- z : topography
- $\mathbf{u} = (u,v)$: velocity vector
- $\mathbf{q} = (q_x, q_y)$: discharge vector

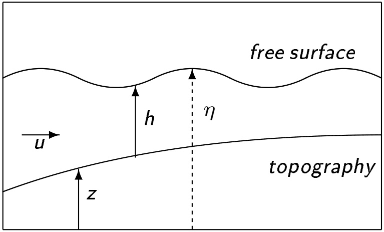

Plan

Pre-balanced formulation

Numerical requirements :

- Preservation of motionless steady states : $\mathbf{u} = 0$ and $\eta = cst$.
- h-positivity preservation.

$\Rightarrow$ "pre - balanced" set of equations [Q. Liang and F. Marche. Numerical resolution of well-balanced shallow water equations with complex source terms. Advances in Water Resources, 2009.]

Main idea : Use η as a conservative variable (instead of h).

Derived formulation for the frictionless model

$$V_t + \nabla \cdot \tilde{H}(V, z) = \tilde{S}(V, z), \qquad with$$

$$V = \begin{pmatrix} \eta \\ q_x \\ q_y \end{pmatrix} \qquad \tilde{H}(V, z) = \begin{pmatrix} q_x & q_y \\ uq_x + \frac{1}{2}g(\eta^2 - 2\eta z) & vq_x \\ uq_y & vq_y + \frac{1}{2}g(\eta^2 - 2\eta z) \end{pmatrix}$$

$$\tilde{S}(V, z) = \begin{pmatrix} 0 \\ -g\eta z_x \\ -g\eta z_y \end{pmatrix}.$$

Semi-discrete finite volume homogeneous scheme

$$|C_i|\frac{d}{dt}V_i + \sum_{k=1}^{\Lambda(i)} \int_{\Gamma_{ij(k)}} \tilde{H}(V,z).\vec{n}_{ij(k)}\, ds = 0.$$

Numerical flux function $\mathcal{H} : (U, V, \vec{n}) \rightarrow \mathcal{H}(U, V, \vec{n})$ derived from 1D scheme (HLL, HLLC, VFroe ...).

- Lipschitz continuous.
- consistent with the exact flux : $\mathcal{H}(U, U, \vec{n}) = \tilde{H}(U).\vec{n}$
- conservation property : $\mathcal{H}(U, V, -\vec{n}) = -\mathcal{H}(V, U, -\vec{n})$

Numerical flux through Γ_{ij}

$$\mathcal{H}_{ij} := \mathcal{H}(V_i^n, V_j^n, z, z, \vec{n}_{ij})$$

Semi - discrete homogeneous scheme

$$|C_i|\frac{d}{dt}V_i + \sum_{k=1}^{\Lambda(i)} l_{ij(k)}\mathcal{H}_{ij(k)} = 0.$$

Modified Riemann states

Modification of the scheme to ensure positivity of h and account the source, even on wet/dry interfaces.

i ("left") and j ("right") Riemann states at the edge Γ_{ij} :

- interface topography value : $\tilde{z}_{ij} = \max(z_i, z_j)$
- wet/dry interface : $\Delta_{ij} = \max(0, \tilde{z}_{ij} - \eta_i)$
- new interface topography value :

$$\bar{z}_{ij} = \tilde{z}_{ij} - \Delta_{ij}$$

→ *Modified* hydrostatic reconstruction (Audusse, 2004)

- non negative reconstruction of h :

$$h^*_{ij} = max(0, \eta_i - \tilde{z}_{ij}),\ h^*_{ji} = max(0, \eta_j - \tilde{z}_{ij})$$

- reconstruction of the free surface :

$$\eta^*_{ij} = h^*_{ij} + \tilde{z}_{ij} - \Delta_{ij},\ \eta^*_{ji} = h^*_{ji} + \tilde{z}_{ij} - \Delta_{ij}$$

New edges values

$$V^*_{ij} = (\eta^*_{ij}, h^*_{ij}\mathbf{u}_i), \quad V^*_{ji} = (\eta^*_{ji}, h^*_{ji}\mathbf{u}_j).$$

Formulation of the first order scheme

Source term : a convenient discretization

$$S_{c,i} = \sum_{k=1}^{\Lambda(i)} \ell_{ij(k)} S_{c,ij(k)} = \sum_{k=1}^{\Lambda(i)} \ell_{ij(k)} \begin{pmatrix} 0 \\ g\hat{\eta}_{ij(k)}(z_i - \overline{z}_{ij(k)})\vec{n}_{ij(k)} \end{pmatrix},$$

where $\hat{\eta}_{ij}$ is an approximation of η at the edge Γ_{ij} ; we take $\hat{\eta}_{ij} = \frac{\eta_i+\eta_j}{2}$.

First order scheme

$$|C_i| \frac{V_i^{n+1} - V_i^n}{\Delta t} + \sum_{k=1}^{\Lambda(i)} l_{ij(k)} \mathcal{H}_s(V_{ij(k)}^*, V_{j(k)i}^*, z_i, z_j, \vec{n}_{ij(k)}) = 0, \quad with$$

$$\mathcal{H}_s(V_{ij}^*, V_{ji}^*, z_i, z_j, \vec{n}_{ij}) = \mathcal{H}(V_{ij}^*, V_{ji}^*, \overline{z}_{ij}, \overline{z}_{ij}, \vec{n}_{ij}) - S_{c,ij}.$$

Main properties

- Well Balancing for motionless steady states.
- Robustness (preservation of the positivity of the water height) under an appropriate CFL.

Numerical gradient approximations

⇒ substitute in the numerical flux function $\mathcal{H}_{ij} = \mathcal{H}(V_i^n, V_j^n, \vec{n}_{ij})$, the values V_i and V_j by "better" interpolations V_{ij} and V_{ji} at the interface Γ_{ij}.
Strategy : [S. Camarri, M.V. Salvetti, B. Koobus, and A. Dervieux. A low-diffusion muscl scheme for les on unstructured grids. Computers and Fluids, 2004.] :

- $\hat{V} = (\eta, q_x, q_y, h)$: augmented vector.
- T_{ij} and T_{ji} are, respectively, the upstream and downstream triangles, from the initial triangulation $\mathcal{T}$, with respect to the edge ij.

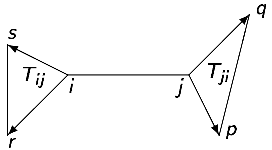

- $\nabla \hat{V}_{T_k}$: P_1 gradient from a continuous and linear interpolation of $\hat{V}$ on the triangle T_k.
- $\nabla \hat{V}_{ij}^{-} = \nabla \hat{V}_{T_{ij}} \cdot \vec{ij}$.
- $\nabla \hat{V}_{ij}^{c} = \hat{V}_j - \hat{V}_i$: centered gradient.
- $\nabla \hat{V}_{ij}^{ho} = \frac{1}{3}\nabla \hat{V}_{ij}^{-} + \frac{2}{3}\nabla \hat{V}_{ij}^{c}$: more accurate way of evaluating the variation of $\hat{V}$.

New edge values

We set : $\mathcal{L}_{ij}(\hat{V}) = \mathcal{L}(\nabla \hat{V}_{ij}^{-}, \nabla \hat{V}_{ij}^{c}, \nabla \hat{V}_{ij}^{ho})$, where $\mathcal{L}$ is a three entries continuous limiter :

$$\mathcal{L}(a,b,c) = \begin{cases} 0 \quad if \quad sgn(a) \neq sgn(b), \\ sgn(a)\min\left(|2a|, |2b|, |c|\right) \quad otherwise \end{cases}$$

Interpolated values on Γ_{ij}

$$\hat{V}_{ij} = \hat{V}_i + \frac{1}{2}\mathcal{L}_{ij}(\hat{V}), \quad \hat{V}_{ji} = \hat{V}_j - \frac{1}{2}\mathcal{L}_{ji}(\hat{V}).$$

Riemann states

- reconstructed values for topography :$z_{ij} = \eta_{ij} - h_{ij}$ *and* $z_{ji} = \eta_{ji} - h_{ji}$
- $\tilde{z}_{ij} = \max\left(z_{ij}, z_{ji}\right), \quad \Delta_{ij} = \max\left(0, \tilde{z}_{ij} - \eta_{ij}\right)$
- new interface topography values : $\bar{z}_{ij} = \tilde{z}_{ij} - \Delta_{ij}$
- water height and free surface reconstruction :

$$h_{ij}^* = \max\left(0, \eta_{ij} - \tilde{z}_{ij}\right), \; h_{ji}^* = \max\left(0, \eta_{ji} - \tilde{z}_{ij}\right)$$
$$\eta_{ij}^* = h_{ij}^* + \tilde{z}_{ij} - \Delta_{ij}, \; \eta_{ji}^* = h_{ji}^* + \tilde{z}_{ij} - \Delta_{ij}$$

Semi-discrete second order finite volume scheme

Reconstructed variable vectors

$$V^*_{ij} = (\eta^*_{ij}, h^*_{ij}\mathbf{u}_{ij}), \quad V^*_{ji} = (\eta^*_{ji}, h^*_{ji}\mathbf{u}_{ji})$$

Source term

$$S_{c,i} = \sum_{k=1}^{\Lambda(i)} \ell_{ij(k)} S_{c,ij(k)} = \sum_{k=1}^{\Lambda(i)} \ell_{ij(k)} \begin{pmatrix} 0 \\ g\hat{\eta}_{ij(k)}(z_i - \bar{z}_{ij(k)})\vec{n}_{ij(k)} \end{pmatrix},$$

$$\text{with } \hat{\eta}_{ij(k)} = (h^*_{ij} + h^*_{ji})/2.$$

Second-order finite volume scheme

$$|C_i|\frac{d}{dt}V_i + \sum_{k=1}^{\Lambda(i)} \ell_{ij(k)}\mathcal{H}_s(V^*_{ij(k)}, V^*_{j(k)i}, z_i, z_j, \vec{n}_{ij(k)}) = 0, \quad with$$

$$\mathcal{H}_s(V^*_{ij}, V^*_{ji}, z_i, z_j, \vec{n}_{ij}) = \mathcal{H}(V^*_{ij}, V^*_{ji}, \bar{z}_{ij}, \bar{z}_{ij}, \vec{n}_{ij}) - S_{c,ij}.$$

$\Rightarrow$ Same discretization as the first order for the source term !

Accuracy validation

$\Rightarrow$ analysis of the scheme's accuracy and convergence rate.

- $\Omega = 20 \times 5$ channel. Splitted grid with $h_n = \frac{20}{n}$, $n = 20, 40, 80, 160$.
- topography : $z(x, y) = 0.8e^{-5(x-10.9)^2 - 50(y-0.5)^2}$.
- inflow boundary (left) : enforced discharge $\mathbf{q} = (4.42, 0)$
  outflow boundary (right) : $\eta = h = 2$.

$\Rightarrow$ Stationary flow for which an exact solution is available.

Convergence rate

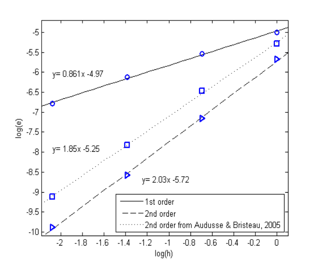

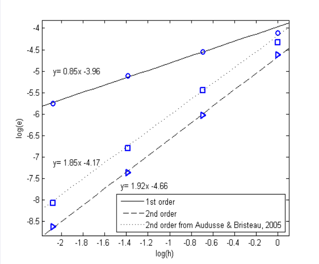

Convergence curves in a logarithmic scale for η (left) and u (right).

Carrier and Greenspan transient solution (1/2)

$\Rightarrow$ behavior of the scheme near wet/dry interfaces.
$\Rightarrow$ accuracy validation : comparison with exact solution and convergence toward a steady state.

- computational domain : $\Omega = [-20, 6] \times [0, 10]$.
- initial condition and time-evolving boundary condition on the left side provided by the exact solution.

Shoreline evolution

204.avi

Carrier and Greenspan transient solution (2/2)

shoreline evolution

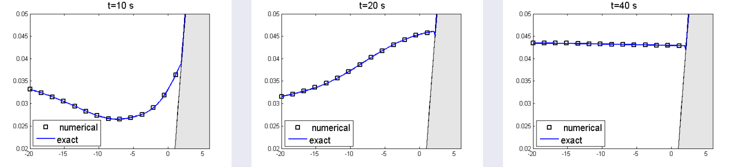

→ Free surface profile at times t=10s, 20s and 40s.

L^1 error analysis

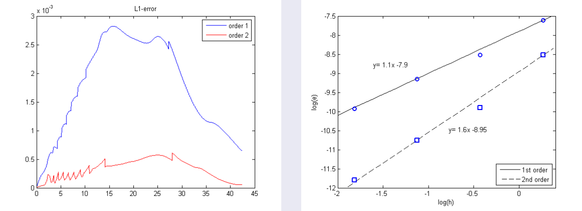

Time series of the L^1 error for first and second order schemes ; $\Delta x = 0.26$ (left). Convergence rate study for increasingly refined regular meshes (right)

Oscillatory flow in a parabolic basin

⇒ 2D test case involving dry areas.
⇒ comparison with an exact solution.

Free surface evolution

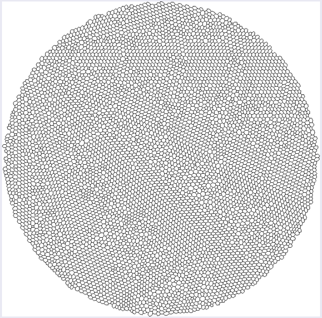

207_1.avi

Comparison with the exact solution

Free surface profile along the x-direction middle section

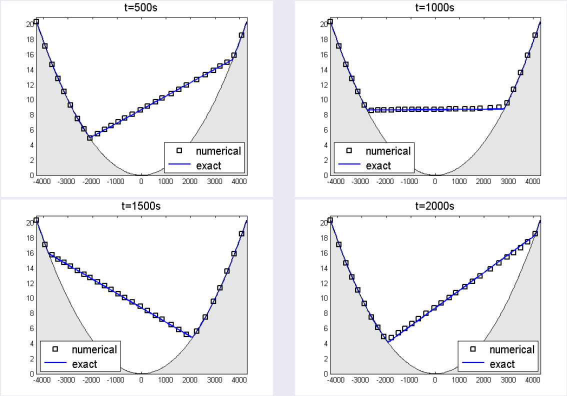

Time history of the free surface at times t=500s, 1000s, 1500s and 2000s.

Small perturbation of a lake at rest (1/3)

$\Rightarrow$ well - balancing property of the first and second order model.

$\Rightarrow$ efficiency of the low diffusion second order reconstruction.

- $\Omega = [0,2] \times [0,1]$ channel. Unstructured triangulation with 11476 nodes.
- topography : $z(x,y) = 0.8e^{-5(x-10.9)^2 - 50(y-0.5)^2}$.
- perturbation of the initial steady state :

$$\eta(x,y,0) = \begin{cases} 1.01 & \text{if } 0.05 < x < 0.15, \\ 1 & \text{elsewhere.} \end{cases}$$

3D surface evolution

205.avi

Small perturbation of a lake at rest (2/3)

Free surface evolution

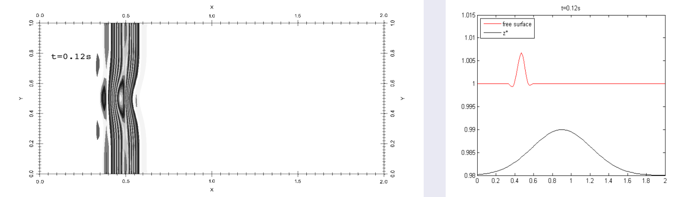

Free surface elevation at t=0.12s : contour and vertical section at y=0.5m.

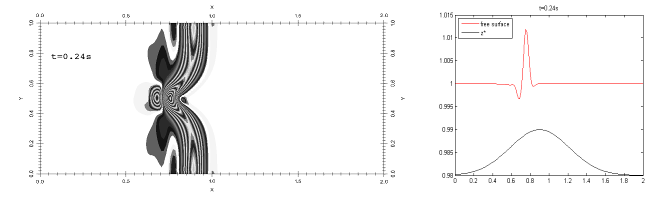

Free surface elevation at t=0.24s : contour and vertical section at y=0.5m.

Small perturbation of a lake at rest (3/3)

Free surface evolution

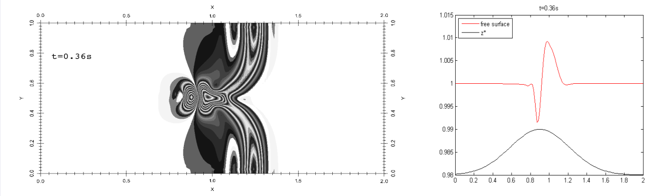

Free surface elevation at t=0.36s : contour and vertical section at y=0.5m.

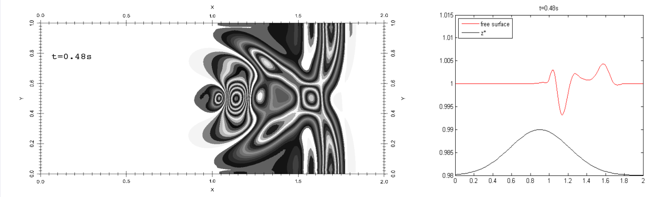

Free surface elevation at t=0.48s : contour and vertical section at y=0.5m.

Malpasset dam break

Reyran river valley (South of France), 1959. Varying topography and complex geometry : benchmark test for dam-break models.

Topography and dual mesh

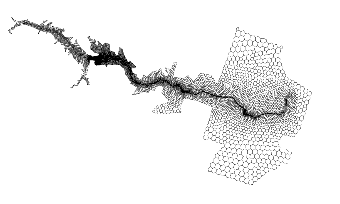

The Malpasset dam break: topography of the river (top) and vertex-centered dual mesh (bottom)

Time series of the water level

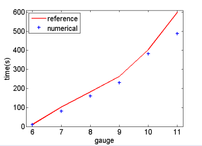

→ **Comparison with experimental data from gauge 6 to 11.**

Plan

The 1D scheme

Main idea : Modification of the intermediate states in the HLL Riemann solver : introduce the friction directly in the intermediate states.

[Berthon C., Marche F., Turpault R. : An efficient scheme on wet/dry transitions for shallow water equations with friction. Computers and Fluids, 2011]

Modified approximated Riemann solver

$$\tilde{U}_{\mathcal{R}}(\tfrac{x}{t}, U_L, U_R) = \begin{cases} U_L \text{ if } \frac{x}{t} \leq a^- \\ U^* + (1-\alpha)\big(U_L^* - U^* - \frac{h^\eta}{\kappa}\mathcal{F}(U_L)\big) \text{ if } a^- \leq \frac{x}{t} \leq 0 \\ U^* + (1-\alpha)\big(U_R^* - U^* - \frac{h^\eta}{\kappa}\mathcal{F}(U_R)\big) \text{ if } 0 \leq \frac{x}{t} \leq a^+ \\ U_R \text{ if } \frac{x}{t} \geq a^+ \end{cases},$$

with

$$U_L(\tfrac{x}{t}, U_L, U_R) = \begin{pmatrix} h^*(\frac{x}{t}, U_L, U_R) \\ h_L u_L \end{pmatrix}, \quad U_R(\tfrac{x}{t}, U_L, U_R) = \begin{pmatrix} h^*(\frac{x}{t}, U_L, U_R) \\ h_R u_R \end{pmatrix}$$

The 1D scheme

New updated values

$$h_i^{n+1} = h_i^n - \frac{\Delta t}{\Delta x}(G^h_{i+\frac{1}{2}} - G^h_{i-\frac{1}{2}})$$

$$(hu)_i^{n+1} = (hu)_i^n - \frac{\Delta t}{\Delta x}\Big[\alpha_{i+\frac{1}{2}} G^{hu}_{i+\frac{1}{2}} - \alpha_{i-\frac{1}{2}} G^{hu}_{i-\frac{1}{2}} -((1-\alpha_{i-\frac{1}{2}})s^{+,u}_{i-\frac{1}{2}} + (1-\alpha_{i+\frac{1}{2}})s^{-,u}_{i+\frac{1}{2}})\Big]$$

- $\alpha_{i+\frac{1}{2}} = \frac{h_{i+\frac{1}{2}}(a_{i+\frac{1}{2}} - a_{i-\frac{1}{2}})}{h_{i+\frac{1}{2}}(a_{i+\frac{1}{2}} - a_{i-\frac{1}{2}}) + q_{i+\frac{1}{2}}\kappa/\Delta x}$

  with $h_{i+\frac{1}{2}} = ((h_i^n)^\eta + (h_{i+1}^n)^\eta)/2$, $q_{i+\frac{1}{2}} = ((hu)_i^n + (hu)_{i+1}^n)/2$

- $s^{-,u}_{i+\frac{1}{2}} = min(0, a^-_{i+\frac{1}{2}})(hu)_i^n - min(0, a^+_{i+\frac{1}{2}})(hu)_{i+1}^n + G^{hu}(U_i^n)$

  $s^{+,u}_{i+\frac{1}{2}} = max(0, a^-_{i+\frac{1}{2}})(hu)_i^n - max(0, a^+_{i+\frac{1}{2}})(hu)_{i+1}^n + G^{hu}(U_i^n)$

$\Rightarrow$ Robustness

Extension to the 2D unstructured case

2D model

$$u_i^{n+1} = \sum_{j \in K_i} \frac{|T_{ij}|}{C_i} \tilde{u}_{ij}^{n+1}, \quad \textit{with}$$

$$\tilde{u}_{ij}^{n+1} = u_i^n - \frac{\Delta t}{|T_{ij}|} l_{ij} \left(\phi(U_i^n, U_j^n, \vec{n}_{ij}) - \phi(U_i^n, U_i^n, \vec{n}_{ij}) \right)$$

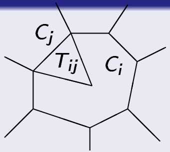

⇒ Natural extension :

1D fluxes at the node i : $G_{i-\frac{1}{2}}$, $G_{i+\frac{1}{2}}$	$\longleftrightarrow$	fluxes of the 3 point scheme on Γ_{ij} : $\phi(u_i^n, u_i^n, \vec{n}_{ij})$, $\phi(u_i^n, u_j^n, \vec{n}_{ij})$

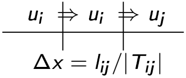

New updated interface contribution vector

$$\tilde{h}_{ij}^n = h_i^n - \frac{l_{ij}\Delta t}{|T_{ij}|} \left(\phi_{ij}^h(u_i^n, u_j^n, \vec{n}_{ij}) - \phi_{ii}^h \right) (u_i^n, u_i^n, \vec{n}_{ij})$$

$$(\tilde{hu})_{ij}^n = (hu)_i^n - \frac{l_{ij}\Delta t}{|T_{ij}|} \Big[\alpha_{ij} \phi^{hu}(u_i^n, u_j^n, \vec{n}_{ij}) - \alpha_{ii} \phi^{hu}(u_i^n, u_i^n, \vec{n}_{ij}) - \left((1-\alpha_{ii}) s_{ii}^{+,u} + (1-\alpha_{ij}) s_{ij}^{-,u} \right) \Big]$$

$$(\tilde{hv})_{ij}^n = (hv)_i^n - \frac{l_{ij}\Delta t}{|T_{ij}|} \Big[\alpha_{ij} \phi^{hv}(u_i^n, u_j^n, \vec{n}_{ij}) - \alpha_{ii} \phi^{hv}(u_i^n, u_i^n, \vec{n}_{ij}) - \left((1-\alpha_{ii}) s_{ii}^{+,v} + (1-\alpha_{ij}) s_{ij}^{-,v} \right) \Big]$$

Second order extension

⇒ Same numerical strategy as the previous scheme :

Augmented vector : $\hat{v} = (\eta, q_x, q_y, h)$.
New interfaces values :

$$\hat{v}_{ij} = \hat{v}_i + \frac{1}{2}\mathcal{L}_{ij}(\hat{v}), \quad \hat{v}_{ji} = \hat{v}_j - \frac{1}{2}\mathcal{L}_{ji}(\hat{v})$$

New values for the flux computation

$$\mathbf{u}_{ij} = \mathbf{q}_{ij}/h_{ij} \quad , \quad u_{ij} = (h_{ij}, h_{ij}\mathbf{u}_{ij})$$

Second order convex combination component

$$\tilde{u}_{ij}^{n+1} = u_i^n - \frac{\Delta t}{|T_{ij}|} l_{ij} \left(\phi(u_{ij}^n, u_{ji}^n, \vec{n}_{ij}) - \phi(u_i^n, u_i^n, \vec{n}_{ij}) \right)$$

Periodic subcritical flow

$\Rightarrow$ convergence toward a steady state ; comparison with analytical solution.
$\Rightarrow$ efficiency of the model near wet/dry transitions.

- $\Omega = 5000 \times 500$ channel. Cartesian splitted grid with $\Delta x = \Delta y = 0.33m$
- steady state for the water height : $h_{ref}(x,y) = \frac{9}{8} + \frac{1}{4} sin(\frac{\pi x}{500})$
- left boundary condition : $h = h_{ref}(0), q_x = 2m.s^{-1}$.
- iterative method for the topography profile computation (see [Delestre O., Marche F. : A numerical scheme for a viscous shallow water model with friction. Journal of Scientific Computing. 2010]).
- Manning-Cheezy friction term : $\eta = 10/3$ and $\kappa = n^2$ with $n = 2$.

Evolution of the free surface

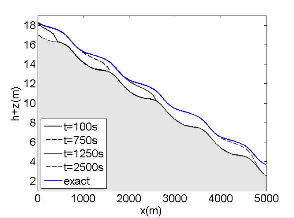

$\rightarrow$ **Time history of the free surface elevation (t=100s, 750s, 1250s, 2500s).**

$\Rightarrow$ Convergence toward the steady state.

Dam - break with friction

$\Rightarrow$ accuracy of the wave speed computation on a flat and wet bottom context.

- computational domain : $\Omega = [-10, 10] \times [0, 4]$. Splitted cartesian grid, with $\Delta x = \Delta y = 0.1$; 8241 nodes.
- initial condition : $h(x, y) = \begin{cases} 1 & \text{if } x < 0, \\ 0 & \text{elsewhere.} \end{cases}$
- approximated solution provided by [Chanson H. Analytical solution of dam break wave with flow resistance. Application to tsunami surges. XXXI IAHR Congress. 2005].
- Darcy formulation for bed friction : $\mathcal{F} = \begin{pmatrix} 0 \\ \frac{f}{8gh}|\mathbf{u}|\mathbf{u} \end{pmatrix}$, with $f = 0.05$.

Time history of the wet/dry interface location

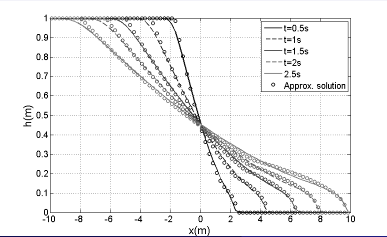

$\rightarrow$ **Water depth profiles on the middle section at t=0, 1, 1.5, 2, 2.5s**

$\Rightarrow$ The evolution of the shoreline seems to be accurately computed.

Moving boundary over a quadratic bottom (1/2)

⇒ accuracy validation : comparison with the exact solution.
⇒ wet/dry interfaces : evolution of the shoreline.

- $\Omega = 4320 \times 500$ basin.
- topography : $z(x,y) = h_0\left(\left(\frac{x}{a}\right)^2 - 1\right)$, with $h_0 = 10$ and $a = 3000$.
- analytical solution available.
- linear friction term : $\mathcal{F} = \begin{pmatrix} 0 \\ \kappa \mathbf{q} \end{pmatrix}$, with $\kappa = 0.001$.

Free surface profiles

215.avi

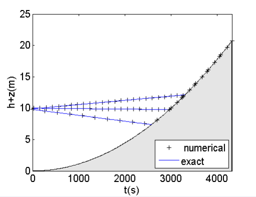

Evolution of the flow and free surface elevation along the x-direction centerline at times t=0s, 300s and 650s.

A new approach for SWE source terms
Arnaud Duran
Governing Equations
Numerical treatment of the topography
Pre-balanced approach
First order scheme
Second order extension
Numerical validations
Accounting frictional terms
The 1D scheme
Second order extension
Numerical validations

Moving boundary over a quadratic bottom (2/2)

Location of the shoreline

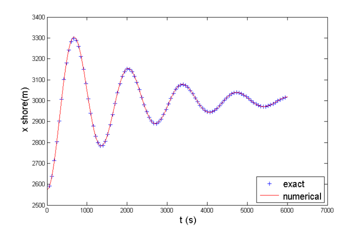

Time series of the wet/dry interface.

shoreline evolution :

$$x = \frac{a^2 e^{-\kappa t/2}}{2gh_0}\left(-Bs\cos(st) - \frac{\kappa B}{2}\sin(st)\right) + a$$

$\Rightarrow$ Excellent agreement with the exact solution.

Error quantification

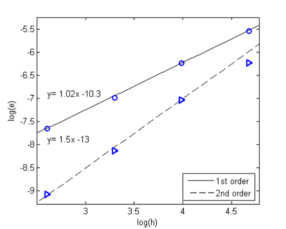

Δx	order1	order2
108	3.92e-3	1.97e-3
54	1.95e-3	8.76-4
27	9.33e-4	2.92e-4
13.5	4.77e-4	1.14e-4

Oscillatory flow in a parabolic bowl (1/2)

[Wang Y., Liang Q., Kesserwani G., Hall J.W. A 2d shallow flow model for practical dam break simulations. J. Hydraulic Research. 2011]
$\Rightarrow$ accuracy validation and behavior on wet/dry transitions in an unstructured context.

- $\Omega = \mathcal{C}(0, 4320)$. Unstructured triangulation with 13674 nodes.
- topography : $z(r) = r^2(h_0/a^2)$, with $h_0 = 10$ and $a = 3000$.
- analytical solution available.
- linear friction term, with $\kappa = 0.002$.

Time history of the free surface

207.avi

Oscillatory flow in a parabolic bowl (2/2)

Free surface profiles

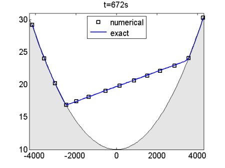

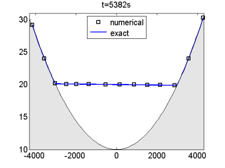

Water surface level along the section x=0 after a half period (left) and four periods (right).

Velocity vector

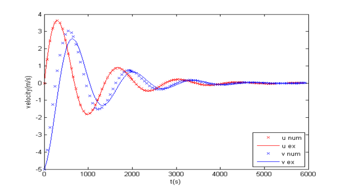

→ **Time series of the velocity components at (1000,0).**

⇒ Numerical prediction and exact solutions are very close. The friction model developed by Wang et al. gives similar results.

Malpasset dam break

Reyran river valley (South of France), 1959. Varying topography and complex geometry : benchmark test for dam-break models.

Topography and dual mesh

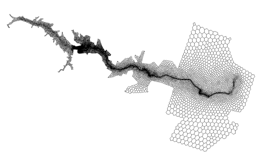

Topography of the river (left) and vertex-centered dual mesh (right).

Time series of the water level

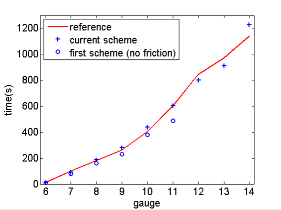

Comparison with experimental data from gauge 6 to 14.

Thank you !